
EXPERIMENTAL INVESTIGATION ON BEHAVIOUR OF CROSS-FLOW THERMAL EFFLUENT DISCHARGE IN FREE SURFACE FLOW

Zulkiflee Ibrahim^{1,*}, Abd. Aziz Abdul Latiff², Noor Baharim
Hashim¹, Herni Halim¹, Nurul Hana Mokhtar Kamal¹,
Nuryazmeen Farhan Haron¹

¹ Department of Hydraulics & Hydrology, Faculty of Civil Engineering Universiti Teknologi
Malaysia, 81310 Skudai, Johor Bahru, Malaysia.

² Department of Water Resources and Environmental Engineering, Faculty of Civil and
Environmental Engineering, Universiti Tun Hussien Onn Malaysia.

*Corresponding Author: zulkfe@utm.my

Abstract: Thermal discharges such as from power stations or industries into rivers causing degradation of water quality. A study was conducted in the laboratory to investigate the changes of the ambient temperature caused by thermal effluent discharged into the flow. A cross-flow thermal effluent is discharged from the bed of the channel. Thermal effluent flow rates of 0.133 liter/s and 0.05 liter/s and ambient flow rates of 20 liter/s and 10 liter/s were used in the study. Observation of thermal mixing process in the channel is concentrated in the near-field zone. The thermal dispersion patterns were observed along the channel through the isothermal lines; while the changes of ambient temperature are studied from the experimental data. The results indicate that the temperature changes are drastic in the near-field mixing zone. Then it gradually reduces along the channel until reaches the far-field mixing zone. Lower layer of the flow experiences high excess temperature compared to middle and upper layers of the flow. Meanwhile, larger effluent flow rate produces higher excess temperature in the receiving water body than small effluent flow rate. Based on experimental data, equations of excess temperature and dispersion were established.

Keywords: *Thermal effluent, multi-port diffuser, cross-flow, dispersion, near-field.*

1.0 Introduction

Hydrothermal pollution is caused by the discharge of thermal effluent into the river which causes a rise in the ambient water temperature (Zimmerman and Geldner, 1978). Apart from giving an adverse effect to the aquatic life, the stability of the river ecosystem will also be endangered. Water used by power plants as coolant where it flows through a device in order to prevent its overheating, transferring the heat produced

by the device to other devices that utilize or dissipate it (Perunding Utama, 2003). It is the cheapest and easiest method of cooling the electric generating plants; withdraw water from a nearby surface water body, pass it through the plant and return the heated water to the same water body.

Excessive heat transferred into the water will typically decrease the concentration of dissolved oxygen in the water (Kim and Il, 1999). This will result in the harming of aquatic life such as amphibians and copepods, increased in metabolic rate in aquatic life. Thus, this aquatic life consuming more food in shorter time compared to normal environment. As the environment changes, the population of aquatic life may decrease as lack of food source and migration and in-migration of aquatic life to a more suitable environment. The food chain may be disrupted as competition for fewer resources happened.

Hence, the best way of discharging the heated effluent into the water body should be designed to minimize the rising of ambient temperature. A study has been carried out to study the impact of the thermal effluent discharge into the water bodies. The main objective of this laboratory study is to investigate the mechanism of heat transport in an open channel flow. In addition, this research is conducted to investigate the impact of thermal discharge in inland water bodies and also the impact of thermal discharge in different ambient flow rates.

The mixing processes are influenced by initial jet characteristic of momentum flux, buoyancy flux and outfall geometry in the near-field zone. Meanwhile buoyant spreading and passive diffusion dominate the mixing process in the far-field (Jirka *et. al.*, 1996). Mixing zones can be classified as near-field and far-field. The study is focused on mixing process in the near-field zone.

2.0 Experimental Implementation

2.1 Model Setup

The experiment is carried out in Hydraulics and Hydrology laboratory, Faculty of Civil Engineering, Universiti Teknologi Malaysia using a 0.3 m wide, 0.3 m deep, and 7.0 m long flume. The layout of the experiment setup is as illustrated in Figure 1. Hot water from a small over-head tank is continuously discharged into open channel flow through PVC pipe with five 12mm diameter ports which acts as a multi-port diffuser system as shown in Figure 2. A red colored dye is added into the hot water to trace the dispersion patterns in the flume. The temperatures in the flow are measured using digital thermometers placed at selected stations along the channel. The multi-port diffuser pipe is placed at the channel bed in a cross-flow direction. The effluent flow rates, Q_e used in the study are 0.133 liter/s and 0.05 liter/s. Meanwhile for the ambient flow rate (Q_a), two different flow rates of 20 liter/s and 10 liter/s are used. The ambient flow rates value selection are based on the capacity of the channel and tank where the full discharge is 20 liter/s and half discharge is 10 liter/s.

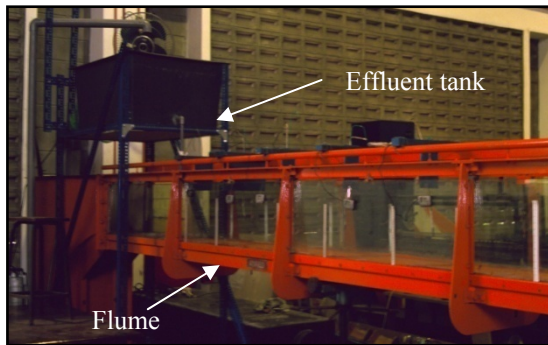


Figure 1: Experimental Model Setup



Figure 2: Multi-port diffuser pipe in cross-flow direction

2.2 Sampling Stations

Mixing flow temperatures are measured at five stations located 480 mm apart along the channel. Digital thermometers are placed at each station and across the channel at three different depths for each ambient flow rate. The sampling depths for ambient flow rate of 20 liter/s are 30 mm, 70 mm and 130 mm from the channel bed. Meanwhile for flow rate, Q_a of 10 liter/s, the depths are 22.9 mm, 53.6 mm and 99.5 mm. Notations used in the experiment are x (longitudinal distance from discharge point), y (transverse system from channel wall), z (vertical distance from channel bed), d (port diameter) and H (total flow depth). The sampling depth values are chosen based on the values of z/d for every sampling station.

2.3 Dimensional Analysis

Three dependent variables selected to describe the heated plume are diameter of port (d) fluid density difference ($\Delta\rho$) and ambient flow velocity (u_a). Temperature difference ΔT obtained in the analysis is normalised to acquire excess temperature, $\Delta T/T_e$ (Kuang and Lee, 2001):

$$\Delta T/T_e = \frac{T_x - T_a}{T_e} \tag{1}$$

where T_a is ambient temperature, T_e is effluent temperature, T_x is observed temperature at distance x along the channel. Using dimensional analysis the relationship for $\Delta T/T_e$ can be written as:

$$\frac{\Delta T}{T_e} = \Phi \left[\frac{x}{d}, \frac{y}{d}, \frac{z}{d}, \frac{Q_a}{Q_e}, \frac{u_a R}{\nu_a}, \frac{u_e d}{\nu_e}, \frac{Ua}{\left(\frac{\Delta \rho}{\rho a} gH \right)^{\frac{1}{2}}} \right] \quad (2)$$

The fifth and sixth terms in equation (2) are Reynolds numbers for ambient and thermal effluent flows, respectively. The last term is defined as densimetric Froude number, F_D . However for this research, the application of densimetric Froude number is not suitable. The reason is the density difference, $\Delta\rho$, between the ambient flow and the effluent is small, the calculated F_D resulted greater than unity thus classified the mixing flow in the flume as supercritical. Thus, the Froude number is used to classify the flow condition.

3.0 Results and Discussion

The analysis of experiment data is focused on the effluent dispersion pattern, spatial excess temperature, dispersion rate, and temporal changes.

3.1 Flow Conditions

Froude number, Fr and Reynolds number, Re are used to determine the ambient flow condition in the experiment. The calculated Fr and Re for both Q_a are given in Table 1.

Table 1: Calculated Fr and Re of the ambient flow in the experimental study.

| Q_a (liter/s) | $Fr = \frac{u}{\sqrt{gH}}$ | $Re = \frac{uR}{\nu}$ |
|-----------------|----------------------------|-----------------------|
| 10 | 0.227 | 21,161 |
| 20 | 0.303 | 37,105 |

The effect of viscosity on flow is determined by using Re . Meanwhile Fr is used to illustrate the effects of gravity on the ambient flow. Turbulent flow occurs when Re is greater than 2000 (Daugherty *et al.*, 1989). The calculated Fr and Re show that the ambient flows are classified as sub-critical with turbulent condition.

Meanwhile, the velocity vectors of the ambient flow can be determined by using Digital Particle Image Velocimetry (DPIV) method. The measuring techniques of DPIV are broadly used to investigate mixing processes related to buoyant jets phenomenon (Davidson, M.J. *et al.*, 2001). DPIV requires the projection of a laser sheet onto the flow field at successive time intervals and the subsequent capturing of the images detailing the position of seeding particles that reflect the laser light. Analysis of the difference in positions of the particles reveals the Lagrangian velocity distribution of the flow field. Through cross-correlation of two successive images in MATLAB software using correlation of URAPIV file, the velocity vectors of the flume are determined. Figure 3 and Figure 4 show the velocity vectors of ambient flows of 20 liter/s and 10 liter/s, respectively. They illustrate that the ambient flow in the channel is in turbulence. This finding supports the calculated Reynolds number described in Table 1.

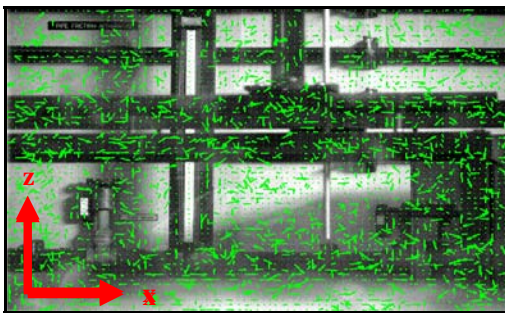


Figure 3: Velocity vectors of ambient flow of Q_a of 20 liter/s using DPIV method

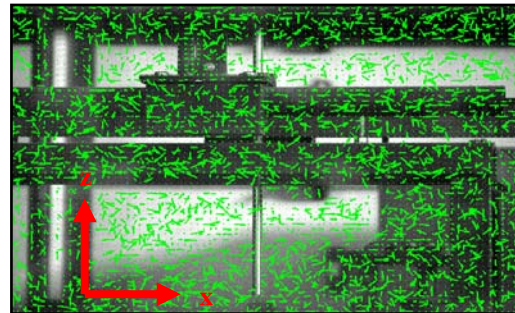


Figure 4: Velocity vectors of ambient flow of Q_a of 10 liter/s using DPIV method

3.2.1 Effluent Dispersion Pattern

The cross-sectional effluent dispersion patterns for cross-flow discharges are illustrated from temperature difference (ΔT) at every station. There are five water temperature measuring stations in the channel for the study. These stations are located at $x_0/d = 0$, $x_1/d = 30$, $x_2/d = 70$, $x_3/d = 110$ and $x_4/d = 150$. Cross-sectioned isothermal lines are plotted to observe the patterns of effluent dispersion patterns the channel.

3.2.1 Dispersion Pattern in Near-Field

Station $x/d = 30$ is selected to study the behaviour effluent dispersion in the near-field region. Figures 5 and 6 show the water temperature difference related to dispersion patterns in the near-field in ambient flow rate of 20 liter/s for Q_e of 0.133 liter/s and Q_e of 0.05 liter/s, respectively. Both figures show that thermal effluent start to disperse in the channel at $x/d = 30$. The movement of the effluent thermal to the top of the channel is influenced by positive buoyancy (Fischer *et al.*, 1979), where heated water with lower density moves upward to the water surface. Higher temperature difference at the bottom of the channel for Q_e of 0.133 liter/s is caused by the larger quantity of thermal effluent discharged into the open channel as compared to for Q_e of 0.05 liter/s. The high water temperature difference in both indicate that lateral mixing process is slower while vertical mixing are almost completed.

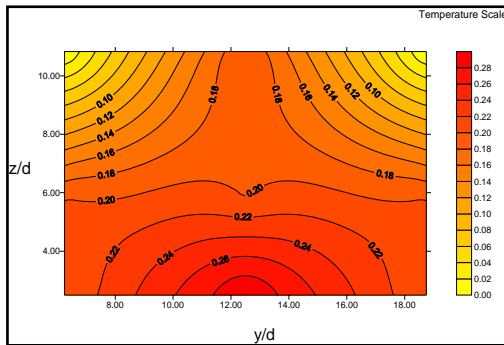


Figure 5: Cross-sectional effluent dispersion pattern (in °C) at $x/d = 30$ for Q_a of 20.0 liter/s for Q_e of 0.133 liter/s

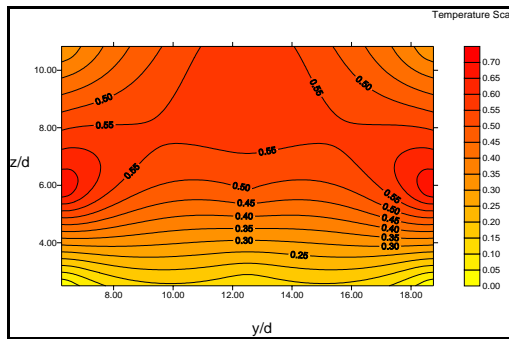


Figure 6: Cross-sectional effluent dispersion pattern (in °C) at $x/d = 30$ for Q_a of 20.0 liter/s for Q_e of 0.05 liter/s

Figure 7 and Figure 8 show dispersion patterns in ambient flow rate of 10 liter/s for Q_e of 0.133 liter/s and Q_e of 0.05 liter/s, respectively. The similar pattern in the near-field region is observed for smaller ambient flow. For Figure 7 the highest temperature remains at the bottom of the channel while for Figure 8 is at the centre of the channel. The movement of the effluent thermal to the top of the channel is influenced by positive buoyancy. For Figure 7, a longer distance is needed to dilute the heated water because the quantity of heated water is larger. Again, the high water temperature difference at that station shows that lateral mixing process is slower in this cross section while vertical mixing is almost completed. The result shows that positive buoyancy accelerates the vertical mixing process in a water body.

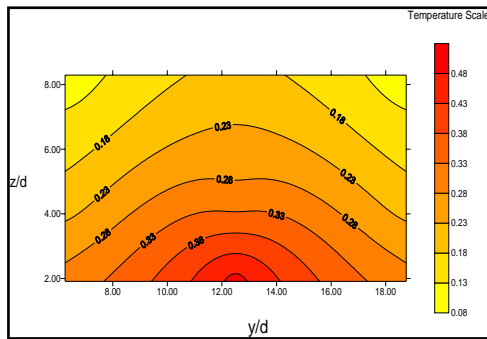


Figure 7: Cross-sectional effluent dispersion patterns (in⁰C) at $x/d = 30$ for Q_a of 10.0 liter/s for Q_e of 0.133 liter/s

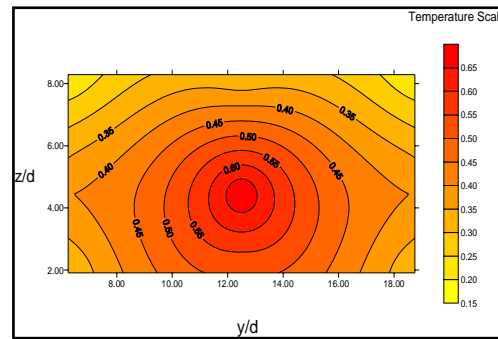


Figure 8: Cross-sectional effluent dispersion patterns (in⁰C) at $x/d = 30$ for Q_a of 10.0 liter/s for Q_e of 0.133 liter/s

3.2.2 Dispersion Pattern in Far-Field

Station $x/d = 110$ is selected to study the behaviour effluent dispersion in the far-field region. Figure 9 and Figure 10 show dispersion patterns at ambient flow rate of 20 liter/s for Q_e of 0.133 liter/s and Q_e of 0.05 liter/s, respectively. Both figures reveals that lateral mixing process at that cross section is nearly completed. In Figure 9 the highest temperature difference of $0.7\text{ }^{\circ}\text{C}$ occurs at the side of the channel due to the lower velocity at channel. Meanwhile in Figure 10, the highest temperature difference occurs at the top of the channel. However, the maximum temperature difference in Figure 10 is smaller than in the Figure 9 which is $0.5\text{ }^{\circ}\text{C}$. This is caused by the quantity of the thermal effluent dispersed into the channel in Figure 10 is smaller ($Q_e = 0.05$ liter/s).

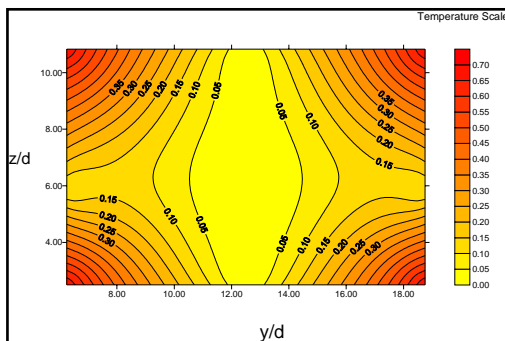


Figure 9: Cross-sectional effluent dispersion patterns (in⁰C) at $x/d=110$ for Q_a of 20.0 liter/s for Q_e of 0.133 liter/s.

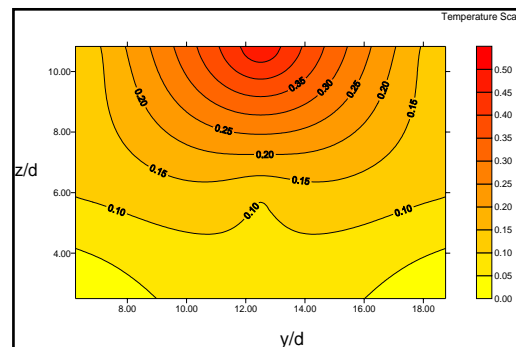


Figure 10: Cross-sectional effluent dispersion pattern (in⁰C) at $x/d = 110$ for Q_a of 20.0 liter/s for Q_e of 0.05 liter/s.

Figure 11 and Figure 12 show dispersion patterns in ambient flow rate of 10 liter/s for Q_e of 0.133 liter/s and Q_e of 0.05 liter/s, respectively. Both figures reveal that lateral mixing process at that cross section is nearly complete. In Figure 11, the highest temperature difference of 1.4 °C occurs at the side of the channel due to the lower velocity at the channel wall. Meanwhile in Figure 12, the highest temperature difference occurs at the top of the channel. However, the maximum temperature difference in Figure 12 is smaller than in the Figure 11 which is 1.0°C. This is caused by the quantity of the thermal effluent dispersed into the channel in Figure 10 is smaller ($Q_e = 0.05$ liter/s).

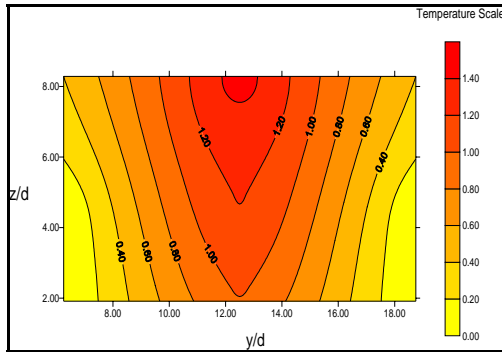


Figure 11 : Cross-sectional effluent dispersion pattern (in °C) at $x/d = 110$ for Q_a of 10.0 liter/s for Q_e of 0.133 liter/s

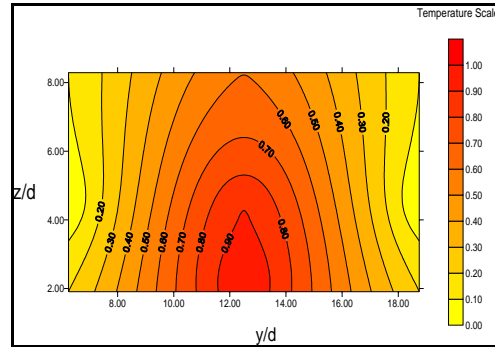


Figure 12 : Cross-sectional effluent dispersion pattern (in °C) at $x/d = 110$ for Q_a of 10.0 liter/s for Q_e of 0.05 liter/s

3.3 Excess Temperature, $\Delta T/T_e$

Analysis on the temperature difference, ΔT is concentrated on two different ambient flow rates, Q_a of 20.0 liter/s and 10.0 liter/s and two different thermal effluent flow rates, Q_e of 0.133 liter/s and 0.05 liter/s. The ratio between the thermal effluent flow rates is 2.67. Subsequently, ΔT obtained in the analysis is normalised to acquire excess temperature, $\Delta T/T_e$ as given in Equation (1). The study on excess temperature is carried out in middle layer of the ambient flow, which is represented by z/H of 0.4.

3.3.1 Effect of Different Q_e on Excess Temperature for a Constant Q_a of 10 liter/s and 20 liter/s

Figure 13 shows longitudinal excess temperature profile for Q_a of 20 liter/s at middle layer of flow. For Q_e of 0.05 liter/s, at x/d of 0, excess temperature is low with zero value because the presence of mass of heated water is not detected. However, as thermal effluent moves further downstream, excess temperature increases indicates that mass of thermal effluent moves upwards. The rising of thermal effluent in the receiving water is

known as positive buoyancy. Then the excess temperature decreases along the channel length as the mixing between thermal effluent and ambient flow continue to take place. For Q_a of 20 liter/s and Q_e of 0.05 liter/s, the relationship for excess temperature in the middle layer of flow is given in Equation (3).

$$\frac{\Delta T}{T_e} = -1.293 \times 10^{-6} \left(\frac{x}{d}\right)^2 + 1.872 \times 10^{-4} \left(\frac{x}{d}\right) + 2.171 \times 10^{-3} \quad (3)$$

Meanwhile for Q_a of 20 liter/s and Q_e of 0.133 liter/s, at x/d of 0, excess temperature is again low because the thermometer does not detect the mass of heated water. However, as thermal effluent moves further downstream, excess temperature increases. Excess temperatures continue to increase due to large quantity of thermal effluent discharges in the channel. The excess temperature for Q_e of 0.133 liter/s at middle layer of flow is as shown in Equation (4).

$$\frac{\Delta T}{T_e} = -2.305 \times 10^{-7} \left(\frac{x}{d}\right)^2 + 86.295 \times 10^{-6} \left(\frac{x}{d}\right) + 6.492 \times 10^{-4} \quad (4)$$

Figure 14 shows longitudinal excess temperature profile for Q_a of 10 liter/s in middle layer of flow. For Q_e of 0.05 liter/s and 0.133 liter/s, at x/d of 0, excess temperature is high because the presence of mass of heated water is not detected. Excess temperature decreases with channel length as mixing between cold ambient water and heated effluent occurs and reduces the mixed water temperature. Excess temperature equations for Q_e of 0.05 liter/s and Q_e of 0.133 liter/s at middle layer of flow are as follow:

$$\frac{\Delta T}{T_e} = 2.58 \times 10^{-6} \left(\frac{x}{d}\right)^2 - 5.909 \times 10^{-4} \left(\frac{x}{d}\right) + 0.037 \quad (5)$$

$$\frac{\Delta T}{T_e} = -1.401 \times 10^{-6} \left(\frac{x}{d}\right)^2 + 3.197 \times 10^{-4} \left(\frac{x}{d}\right) + 16.79 \times 10^{-3} \quad (6)$$

As a conclusion, a lower Q_a produces a higher excess temperature in the receiving water body than higher Q_a .

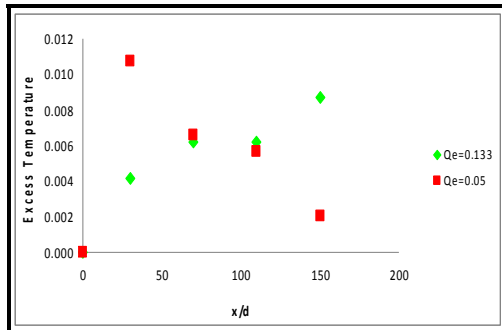


Figure 13: Longitudinal excess temperature profile, $\Delta T/T_e$ for Q_a of 20.0 liter/s in middle layer of flow for different Q_e .

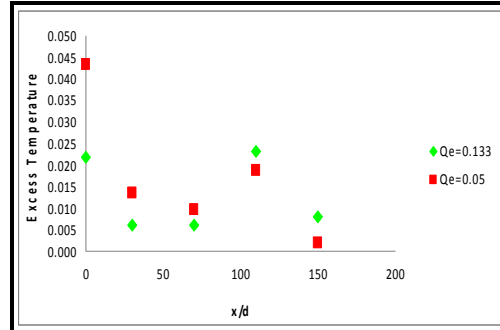


Figure 14: Longitudinal excess temperature profile, $\Delta T/T_e$ for Q_a of 10.0 liter/s in middle layer of flow for different Q_e .

3.3.2 The Effect of Q_a on Excess Temperature

Figure 15 shows longitudinal excess temperature profile for Q_e of 0.133 liter/s in middle layer of flow. For Q_a of 20 liter/s, excess temperature is low with zero value the mass of heated water is not detected by the thermometer. However, as thermal effluent moves further downstream, the excess temperature increases since the thermal mass moves upwards. Excess temperatures keep increasing as a result of the large thermal effluent quantity discharged in the channel. For Q_a of 10 liter/s, at x/d of 0, since the ambient flow rate is lower, excess temperature is high because the presence of mass of heated water is detected. Excess temperature decreases with channel length when mixing occurs between the ambient flow and the thermal effluent.

Figure 16 shows longitudinal excess temperature profile for Q_e of 0.05 liter/s at middle layer of flow. For Q_a of 20 liter/s, at x/d of 0, excess temperature is low. However, as thermal effluent moves further, excess temperature increases as the thermal effluent moves upwards. Positive buoyancy is indicated by the rising of thermal effluent in the flume. Then, the excess temperature decreases with the channel length as mixing between thermal effluent and ambient flow occurs. Meanwhile, for Q_a of 10 liter/s, at x/d of 0, since the ambient flow rate is lower, excess temperature is high because the presence of mass of heated water is detected. Excess temperature decreases with channel length as mixing occurs between ambient flow and thermal effluent, thus reducing the water temperature. It can be concluded that, excess temperatures for low ambient flow rates are higher compared to high ambient flow rate due to less volume of cold water to cool the heated water mass.

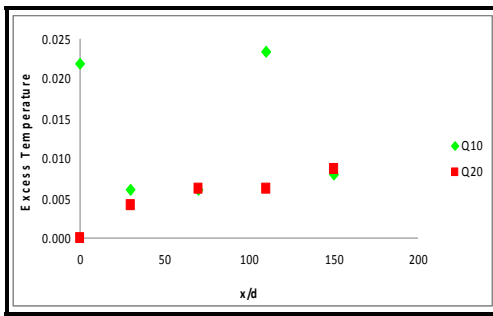


Figure 15: Longitudinal excess temperature profile, $\Delta T/T_e$ for Q_e of 0.133 liter/s at middle layer of flow for different Q_a .

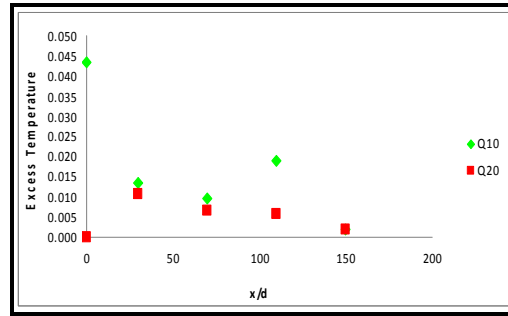


Figure 16: Longitudinal excess temperature profile, $\Delta T/T_e$ for Q_e of 0.05 liter/s at middle layer of flow for different Q_a .

The analysis of dispersion rate is carried out in three different flow depths known as lower layer, middle layer and upper layer of the flow. Lower layer of the flow represents the depth z/H of 0.2 while middle layer corresponds to z/H of 0.4. Meanwhile, upper layer represents z/H of 0.8. Ambient flow velocity and distance from multiport diffuser influence the effluent dispersion rate in open channel flow. The dispersion rate, K_T is calculated using Equation (7) given by Pinheiro *et al.* (1997).

$$K_T = \frac{T_e - T_a}{T_x - T_a} \tag{7}$$

3.4.1 The Effect of Q_e on Dispersion Rate

Figure 17 shows longitudinal dispersion rate profile for Q_a of 20 liter/s in middle layer of flow. Again, for Q_e of 0.05 liter/s and 0.133 liter/s, the momentum ratio between ambient flow and thermal effluent discharged increases because the excess temperature decreases along the channel length. Momentum is defined as the product of the mass of a body and its velocity. The momentum ratio is the ratio between the momentum of effluent and momentum of the ambient flow. As momentum ratio increases, dispersion rate also increases. The dispersion rate for Q_e of 0.05 liter/s is higher than dispersion rate for Q_e of 0.133 liter/s. This is due to momentum ratio for Q_e of 0.05 liter/s is higher than momentum ratio for Q_e of 0.133 liter/s. Equations (8) and (9) show dispersion rate equations for Q_e of 0.05 liter/s and 0.133 liter/s at middle layer of flow respectively.

$$K_T = 8.09 \times 10^{-3} \left(\frac{x}{d}\right)^2 - 52.216 \times 10^{-3} \left(\frac{x}{d}\right) + 13.696 \tag{8}$$

$$K_T = -10.801 \times 10^{-3} \left(\frac{x}{d}\right)^2 + 1.762 \left(\frac{x}{d}\right) + 22.233 \quad (9)$$

Figure 18 shows longitudinal dispersion rate profile for Q_a of 10 liter/s at middle layer of flow. For Q_e of 0.05 liter/s and 0.133 liter/s, as the excess temperatures decreases along the channel length, the momentum ratio increases. Momentum ratio is proportional to dispersion rate. The rising of momentum ratio influence the rising of dispersion rate. The dispersion rate for Q_e of 0.05 liter/s are higher compared to dispersion rate for Q_e of 0.133 liter/s because the momentum ratio for Q_e of 0.05 liter/s is higher compared to momentum ratio for Q_e of 0.133 liter/s. The dispersion rate equations for Q_e of 0.05 liter/s and Q_e of 0.133 liter/s at lower layer of flow for Q_a of 10 liter/s are as follow:

$$K_T = 2.58 \times 10^{-6} \left(\frac{x}{d}\right)^2 - 5.909 \times 10^{-4} \left(\frac{x}{d}\right) + 0.037 \quad (10)$$

$$K_T = -4.037 \times 10^{-3} \left(\frac{x}{d}\right)^2 + 0.63 \left(\frac{x}{d}\right) + 38.283 \quad (11)$$

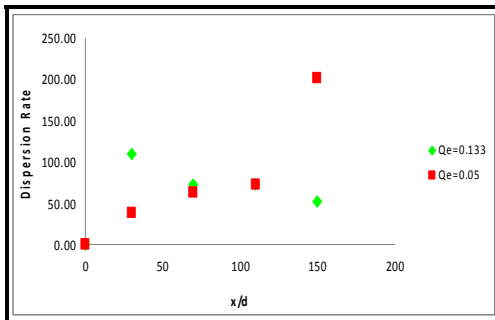


Figure 17 : Longitudinal dispersion rate profile, K_T for Q_a of 20.0 liter/s at middle layer of flow for different Q_e .

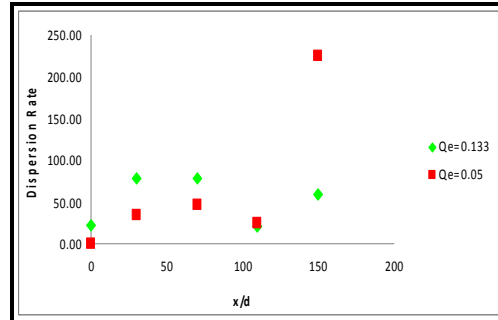


Figure 18: Longitudinal dispersion rate profile, K_T for Q_a of 10.0 liter/s at middle layer of flow for different Q_e .

Figure 19 shows longitudinal dispersion rate profile for Q_e of 0.133 liter/s in middle layer of flow. For Q_a of 20 liter/s and 10 liter/s, as the excess temperature decreases along the channel length, the momentum ratio increases. The rising of momentum ratio

influence the rising of dispersion rate. The dispersion rate for Q_a of 20 liter/s is higher than dispersion rate for Q_a of 10 liter/s because its higher momentum ratio.

Figure 20 shows longitudinal dispersion rate profile for Q_e of 0.05 liter/s at middle layer of flow. Again, excess temperature is inversely proportional to the momentum ratio. As the excess temperature decreases along the channel length, the momentum ratio increases. The rising of momentum ratio influence the rising of dispersion rate. The dispersion rate for Q_a of 20 liter/s is higher compared to dispersion rate for Q_a of 10 liter/s because the momentum ratio for Q_a of 20 liter/s is higher than momentum ratio for Q_a of 10 liter/s.

In general, as thermal effluent is discharged in the channel, the dispersion rates for higher ambient flow rate are higher compared to dispersion rate for lower ambient flow rate in high thermal effluent flow rate because the momentum ratio for higher ambient flow rate is higher compared to momentum ratio for lower ambient flow rate.

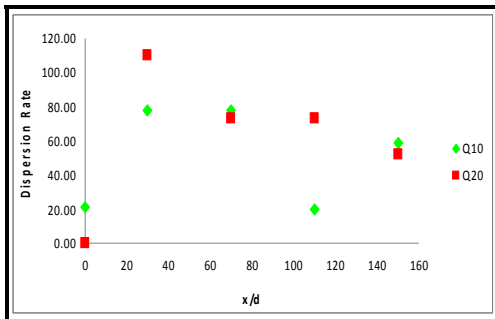


Figure 19 : Longitudinal dispersion rate profile, K_T for Q_e of 0.133 liter/s at middle layer of flow for different Q_a .

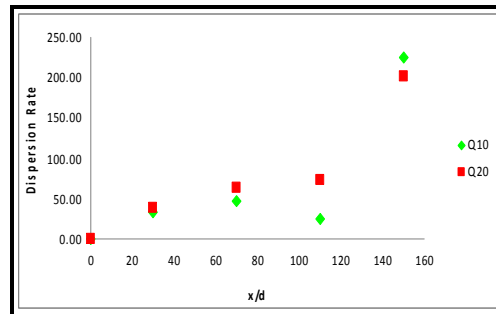


Figure 20 : Longitudinal dispersion rate profile, K_T for Q_e of 0.05 liter/s at middle layer of flow for different Q_a .

3.5 Temporal Pattern of Ambient Temperature Differences, ΔT

The dimensionless time, t^* is used in the analysis in which t^* is equal to:

$$t^* = \frac{t}{t_e} \tag{12}$$

where t is time recorded in the experiment while t_e is total time taken to discharge thermal effluent into the channel (in this study, $t_e=210$ seconds). Discussion is focused on z/H of 0.4 and y/d of 12.5 for both Q_a of 20 liter/s and 10 liter/s.

Figures 21 and 22 show maximum temperature difference recorded at x/d of 30 which is located in the near-field region. This condition happens because station x/d of 30 is located near to the diffuser pipe and experiences the high temperature of heated water. At x/d of 110, heated water has mixed with ambient water therefore the maximum temperature difference is less than temperature difference at x/d of 30. Both figures show when t^* is larger than 1, the temperature difference decreases as the loading of heated water into ambient flow is stopped.

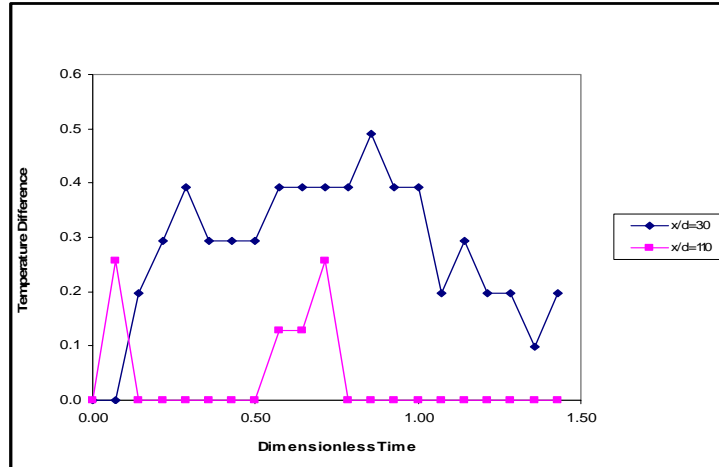


Figure 21: Temporal changes of temperature difference for Q_a of 20 liter/s at x/d of 30 and x/d of 110

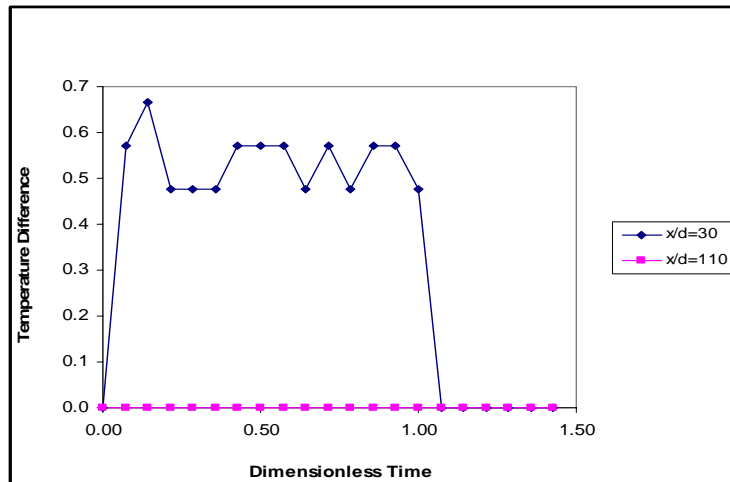


Figure 22: Temporal changes of temperature difference for Q_a of 10 liter/s at x/d of 30 and x/d of 110

3.0 Conclusions

Thermal effluent discharge into open channel flow is a complex process since it deals with turbulence, density difference and heat loss in the receiving water body. However, this research gives some basic understandings on the thermal effluent mixing process. Conclusions that can be drawn from the experimental investigation on behaviour of thermal effluent in free surface flow are:

- (i) Positive buoyancy occurs when thermal effluent is discharged into ambient flow at the bottom of the channel. The heated mass moves upward to the water surface as the density of heated water is lower than ambient water.
- (ii) The thermal effluent disperses uniformly and cools gradually when it moves further from the discharge point.
- (iii) Higher excess temperature is produced by larger effluent volume and lower ambient flow rates. Lower layer of the flow experiences higher excess temperature than middle and upper layer of the flow near the discharge point.
- (iv) Higher dispersion rate is produced by smaller volume of thermal effluent flow and higher volume of ambient flow due to higher momentum ratios.
- (v) Some empirical equations are established on the profiles of excess temperature and dispersion rate along the open channel flow.

5.0 Acknowledgement

The financial of this research was supported by Research Management Centre (RMC), UTM and the Ministry of Higher Education (MOHE) under FRGS vote no. 78123. The authors are indebted to all Hydraulics and Hydrology laboratory technical staffs for their assistance and research students who involved directly in the experimental work. Two anonymous reviewers are thanked for their helpful and constructive criticism.

6.0 References

- Adams, E.E. (1982). Dilution Analysis for Unidirectional Diffusers, *Journal of Hydraulic Division*, ASCE, Vol.108. No. HY3. 327-342.
- Afidah Murni Sakri, Roosaneza Ramli, Zulkiflee Ibrahim, Ruzanna Ahmad Zahir and Rosmunira Zukkaflī (2005). Laboratory Investigation on Co-flow and Crossflow Thermal Effluent Discharge in Open Channel Flow, *Proceeding SEPKA 2005*. 184-192.
- Brennen, C.E. (2005). *Fundamentals of Multiphase Flow*. New York: Cambridge University Press.
- Chow, V.T. (1959). *Open Channel Hydraulics*. Tokyo: McGraw-Hill. 7-14.
- Daugherty, R.L, Franzini, J.B., Finnemore, E.J. (1989). *Fluid Mechanics with Engineering Applications*. Singapore: Mc Graw-Hill. 340-364.
- Davidson, M.J., Gaskin, S. and Wood, I.R. (2001). A Study of A Buoyant Axisymmetric Jet in a Small Co-Flow. *Journal of Hydraulic Research*, Vol. 40. No. 4. 477-489.

- Fischer, H.B., List, E.J., Koh, R.C.Y., Imberger, J., Brooks, N.H. (1979). *Mixing in Inland and Coastal Waters*. San Diego, California: Academic Press. 105-145.
- Jirka, G.H., Robert, L.D. and Steven, W.H. (1996). *User's Manual for CORMIX: A Hydrodynamic Mixing Zone Model and Decision Support System for Pollutant Discharge into Surface Waters*. United States of America: U.S. EPA. 152.
- Kim, D.G. and Il, W.S. (1999). Modelling the Mixing of Heated Water Discharged from a Submerged Multiport Diffuser. *Journal of Hydraulic Research*. Vol. 38. 259-269.
- Kuang, C.P and Lee, J.H.W. (2001). Effect of Downstream Control on Stability and Mixing of a Vertical Plane Jet in Confined Depth. *Journal of Hydraulic Research*. Vol. 39. No. 4. 375-391.
- Lee, J.H.W. and Chu, V.H. (2003). *Turbulent Jets and Plumes-A Lagrangian Approach*. USA: Kluwer Academic Publishers. 211-247.
- Martin, J.L. and McCutcheon, S.C. (1999). *Hydrodynamics and Transport for Water Quality Modeling*. Boca Raton: CRC Press, Inc. 91-92.
- Perunding Utama Sdn. Bhd. (2003). *Detailed Environmental Impact Assessment for Proposed 3 x 700 MW Coal-Fired Power Plant at PTD 707 & 708, Tanjung Bin, Mukim Serkat, Daerah Pontian, Johor Darul Takzim*. Vol 2. unpublished.
- Pinheiro, A.C.F.B and J.P. Ortiz. (1997), *Comparative Analysis of Heated Water Dispersion in Stillwater Body Using Software CORMIX 1, PHOENICS and PLUMAC 2.2*. xxii IAHR Congress.
- Rodi, W. (1982) *Turbulent Buoyant Jets and Plumes*. Great Britain: Pergamon Press Ltd.
- Stefan H.G. and Hondzo, M. (1996). Heat Transport. in: Singh, V.P. and Hager, W.H. (eds.) *Environmental Hydraulics*. Netherlands: Kluwer Academic Publishers. 189-218.
- Zimmerman and Geldner (1978). Thermal loading of River Systems. in: Zoran, P.Z. *Thermal Effluent Disposal from Power Generation*. Washington: Hemisphere Publishing Corporation. 175-194.